

Cutting Forces Modeling Considering the Effect of Tool Thermal Property – Application to CBN Hard Turning

Yong Huang, Research Assistant
Steven Y. Liang, Professor
George W. Woodruff School of Mechanical Engineering
Georgia Institute of Technology
Atlanta, GA 30332-0405, USA

Abstract

Force modeling in metal cutting is important for a multitude of purposes, including thermal analysis, tool life estimation, chatter prediction, and tool condition monitoring. Numerous approaches have been proposed to model metal cutting forces with various degrees of success. In addition to the effect of workpiece materials, cutting parameters, and process configurations, cutting tool thermal properties can also contribute to the level of cutting forces. For example, a difference has been observed for cutting forces between the use of high and low CBN content tools under identical cutting conditions. Unfortunately, among documented approaches, the effect of tool thermal property on cutting forces has not been addressed systemically and analytically. To model the effect of tool thermal property on cutting forces, this study modifies Oxley's predictive machining theory by analytically modeling the thermal behaviors of the primary and the secondary heat sources. Furthermore, to generalize the modeling approach, a modified Johnson-Cook equation is applied in the modified Oxley's approach to represent the workpiece material property as a function of strain, strain rate, and temperature. The model prediction is compared to the published experimental process data of hard turning AISI H13 steel (52 HRC) using either low CBN content or high CBN content tools. The proposed model and finite element method both predict lower thrust and tangential cutting forces and higher tool-chip interface temperature when the lower CBN content tool is used, but the model predicts a temperature higher than that of the finite element method.

Nomenclature

a_{chip}	Thermal diffusivity of chip
c	Strain rate constant
c_{heat}	Heat capacity of workpiece (and chip)
C, B, D, E, m, n	Parameters in modified Johnson-Cook equation
$B(x)$	Fraction of secondary heat source transferred into the chip
F	Frictional force at tool-chip interface
F_c	Cutting force
F_t	Thrust force
F_N	Normal force on AB

F_S	Shear force on AB
h	Plastic tool-chip contact length
I	Parameter defined in Appendix A
k_{AB}	Shear flow stress along AB
k_{ch}	Shear flow stress along tool-chip interface
k_{chip}	Thermal conductivity of chip
k_{tool}	Thermal conductivity of tool
K_0	Zero order Bessel function
l	Length of AB, that is, length of shear band
T	Measured or estimated temperature
$T_{chip - shear}$	Temperature rise on the chip side
$T_{interface-ave}$	Average temperature rise along the tool-chip interface
T_m	Melting point temperature
T_0	Room temperature
T_r	Reference temperature for measuring σ_0
$T_{shear-ave}$	Average temperature rise along the primary shear zone
$T_{tool-friction}$	Temperature rise on the tool side
N	Normal force at tool-chip interface
$q_{frictional}$	Secondary heat source intensity
q_{shear}	Primary shear heat source intensity
R	Resultant cutting force
t	Undeformed chip thickness
t_{ch}	Chip thickness
V	Cutting velocity
V_s	Shear velocity
V_{chip}	Chip velocity
w	Depth of cut
x,y,z,X,Y,Z'	The coordinates of the points used in temperature calculation
α	Rake angle
γ	Shear strain
γ_{AB}	Shear strain rise up to plane AB
$\dot{\gamma}_{AB}$	Shear strain rate along AB
$\dot{\gamma}_{int}$	Shear strain rate along tool-chip interface
δ	Ratio of thickness of tool-chip interface plastic zone to chip thickness
ε	Uniaxial (effective) strain
$\dot{\varepsilon}$	Strain rate
$\dot{\varepsilon}_0$	Reference strain rate (for convenience, be made equal to 1)
λ	Frictional angle between R and N
ρ	Density

θ	Angle of inclination of the resultant cutting force R to shear zone AB
σ_0	Flow stress at reference temperature T_r
σ_N	Average normal stress at tool-chip interface
σ'_N	Normal stress at tool-chip interface from boundary condition at B determined from stress distribution along AB
τ_{int}	Resolved shear stress at tool-chip interface
ϕ	Shear angle
ψ	Inclination of slipline to some fixed axis

1. Introduction

Force modeling in metal cutting is important for thermal analysis, tool life estimation, chatter prediction, and tool condition monitoring purposes. Significant efforts have been devoted to understanding the force profiles in metal cutting. Along with a laborious experimental approach, several numerical and analytical approaches have been proposed to model the chip formation forces and the associated cutting forces. Finite element method (FEM) has been applied to simulate machining process since the early 1970's [KLAM73]. After that time, FEM with different derivatives has received widespread attention in the numerical modeling of machining processes [WANG88] [NGEG99]. Although some successes have been gained in modeling the chip formation forces in metal cutting by FEM, it is not yet ready to be applied due to the fact that it is laborious and not very easily extended to practical 3-D turning cases.

Analytical models have been favored for the modeling of forces in metal cutting because they are easy to implement and can give much more insight about the physical behavior in metal cutting. To model the chip formation forces in metal cutting, two fundamental approaches have been extensively researched: minimum energy principle [MERC45] [LEEE51] and slip line field theory [OXLE89]. The former assumes that the plastic deformation occurred uniformly in the shear plane only so that the cutting energy can be calculated from the shear strain and stress at the shear plane. Minimizing this energy with respect to the shear angle yields the direction of the shear plane [MERC45] [LEEE51]. Unfortunately, the solutions did not take into account factors such as flow stress varying with temperature, strain, and strain rate. Alternatively, by using plasticity theory for the plane strain case, slip line fields are constructed around the primary shear zone from experiments, and also by considering the effects of strain, strain rate and temperature on the flow stress a parallel-sided shear zone approach, which was presented by Oxley [OXLE89]. Numerous researchers have applied or modified these two approaches to model the force profiles afterwards in metal cutting.

Force difference is observed when using the same type of tools, but with different thermal properties. For example, under the same cutting condition there is force difference between using high and low CBN content tools, which are commonly used in turning hard steels. Unfortunately, among the documented approaches, the effect of tool thermal property on cutting forces has not been addressed analytically. It is generally recognized that low CBN content tools have longer life than those of high CBN content tools in hard turning. Several mechanisms are discussed for this phenomenon [KONI93] [BARR01]. Unfortunately, no effort has been made to take into

account the effect of tool CBN content on chip formation process as of yet, although the stress and temperature distributions are considered the main factors in determining tool wear rate. Better analytical understanding of the effect of tool thermal property on chip formation process can help to improve the modeling of tool wear rate in hard turning.

The objective of this paper is to model the effect of tool thermal property on cutting forces. In this paper, instead of using empirical equations in estimating temperature of primary and secondary shear zones, modification to Oxley’s predictive machining theory [OXLE89] is attempted by analytically describing the primary and secondary heat source behaviors. Temperature distribution along the primary and secondary shear zones is modeled by using moving heat source method [HUAN02]. Furthermore, in order to generalize the modeling approach, a modified Johnson-Cook equation is applied in the chip formation model to represent the workpiece material properties as a function of strain, strain rate, and temperature. The proposed approach can express the effect of tool thermal property on cutting forces considering the cutting parameters and configurations. For validation, the model predictions are compared to the published experimental process data of hard turning AISI H13 steel (52 HRC) [NGEG99] using either low CBN content or high CBN content tools.

2. Force Modeling in 2-D Metal Cutting

2.1. Basic assumptions and cutting geometric model

The assumptions used herein to simplify the modeling of metal cutting are: (1) Cutting process is orthogonal. (2) No heat loss along the primary/secondary heat zones. (3) Uniform normal stress/shear stress distributions along the tool-chip interface. (4) Preheating effect is negligible.

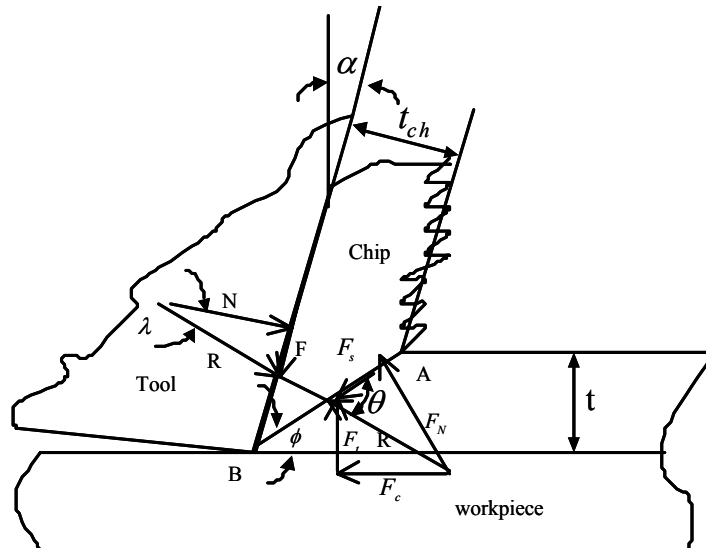


Fig. 1. Cutting geometric model in metal cutting

As shown in Fig. 1, the basic force relationships can be given as:

$$t_{ch} = \frac{t \cos(\phi - \alpha)}{\sin \phi} \quad (1)$$

$$F_c = R \cos(\lambda - \alpha), F_t = R \sin(\lambda - \alpha), F_s = k_{AB} l w \quad (2)$$

$$F = R \sin \lambda, N = R \cos \lambda \quad (3)$$

$$R = \frac{F_s}{\cos \theta} = \frac{k_{AB} t w}{\sin \phi \cos \theta} \quad (4)$$

2.2. Thermal modeling of the primary and secondary heat sources

Two main heat sources are considered: primary heat source along the primary shear zone, and secondary heat source along the tool-chip interface. Referring to the proposed thermal model in turning process [HUAN02], temperature rise on the chip side is attributed to the primary and secondary heat sources, and that on the tool side is attributed to the secondary heat source. Primary heat source contributes to the temperature distribution on the tool side indirectly by affecting the heat partition ratio along the tool-chip interface. In modeling the turning process, it is commonly assumed the stresses are uniformly distributed along the tool-chip interface to simplify the problem [OXLE89]. The corresponding heat source along the tool-chip interface is considered uniform in this modeling approach. Here for the chip side, the effect of the primary shear zone is modeled as a uniform moving oblique band heat source, and that of the secondary shear zone as a uniform moving band heat source within a semi-infinite media. For the tool side, the effect of the secondary heat source is modeled as a uniform static rectangular heat source within a semi-infinite media.

As documented in [HUAN02], the temperature rise along the shear zone (X, Z) can be calculated as:

$$\begin{aligned} T_{chip-shear}(X, Z) = & \frac{q_{shear}}{2\pi k_{chip}} \int_0^l e^{-\frac{(X-X_i)V_{chip}}{2a_{chip}}} \\ & \left\{ K_0 \left(\frac{V_{chip}}{2a_{chip}} \sqrt{(X-X_i)^2 + (Z-Z_i)^2} \right) \right. \\ & + \frac{1}{2} K_0 \left(\frac{V_{chip}}{2a_{chip}} \sqrt{(X-X_i)^2 + (2t_{ch} - Z - Z_i)^2} \right) \\ & \left. + \frac{1}{2} K_0 \left(\frac{V_{chip}}{2a_{chip}} \sqrt{(X-X_i)^2 + (Z+Z_i)^2} \right) \right\} dl_i \quad (5) \end{aligned}$$

where $X_i = l - li \sin(\phi - \alpha)$, $Z_i = li \cos(\phi - \alpha)$, and $l = t_{ch} / \cos(\phi - \alpha)$. The temperature rise along the tool-chip interface (X, Y, Z') is

$$T_{tool-friction}(X, Y, Z') = \frac{1}{2\pi k_{tool}} \int_0^h [1 - B(x)] q_{frictional} dx \int_{-b}^b \left(\frac{1}{R_i} + \frac{1}{R'_i} \right) dy \quad (6)$$

where $R_i = \sqrt{(X-x)^2 + (Y-y)^2 + Z'^2}$, $R'_i = \sqrt{(X-2h+x)^2 + (Y-y)^2 + Z'^2}$, and $B(x)$ is the heat partition ratio of the secondary heat source going to the chip side. The ratio $B(x)$ can be solved [HUAN02] based on a well-adopted assumption: temperature rise on the chip side and on the tool side along the interface should be the same.

The heat intensity of the primary and secondary heat sources in this study is considered uniform and can be computed as

$$q_{shear} = \frac{F_s V_s}{lW}, \quad q_{frictional} = \frac{FV_{chip}}{hW} \quad (7)$$

Based on the temperature rise profiles along the primary shear zone and tool-chip interface, the average temperature can be calculated respectively as follows:

$$T_{shear-ave} = \frac{\int_0^l T_{chip-shear}(X, Z) dl}{l} + T_0, \quad T_{interface-ave} = \frac{\int_0^{h_n} T_{tool-friction}(X, 0, 0) dX}{h} + T_0 \quad (8)$$

The calculated average temperature is used to compute the flow stress along the primary shear zone and at the tool-chip interface.

2.3. Constitutive equation of workpiece material

In Oxley's predictive machining theory, the velocity-modified temperature T_{mod} is calculated from Equ. (9) to account for the strain rate and temperature effects on the material properties. Piecewise, high order curve fitting equations for low carbon steel are used to describe the relationship between modified temperature T_{mod} and both flow stress σ_0 and strain-hardening index n [OXLE89]. Accordingly, the shear stress can be determined by Equ. (10) as discussed in [OXLE89]. Unfortunately, for only a few low carbon steels is such a documented relationship available. For high carbon content steel or their hardened products, such as AISI H13 steel and (hardened) 52100 bearing steel, there are no such available documented constitutive equations that are required as the inputs for Oxley's predictive machining theory.

$$T_{mod} = T[1 - 0.09 \lg(\dot{\epsilon})] \quad (9)$$

$$k = \frac{\sigma}{\sqrt{3}} = \frac{\sigma_0 \epsilon^n}{\sqrt{3}} \quad (10)$$

To generalize Oxley's modeling approach, there is a need to model workpiece material properties with a more general constitutive law, which is easy to be determined. The Johnson-Cook equation as Equ. (11) and the modified Johnson-Cook equation [SHAT00] as Equ. (12) are

adopted in this study to represent the material flow stress behavior under the machining condition.

$$\sigma = \left(\sigma_0 + B\phi^n \right) \left(1 + C \ln \left(\frac{\dot{\epsilon}}{\dot{\epsilon}_0} \right) \right) \left(1 - \left(\frac{T - T_r}{T_m - T_r} \right)^m \right) \quad (11)$$

$$\sigma = \left(\sigma_0 + B\phi^n \right) \left(1 + C \ln \left(\frac{\dot{\epsilon}}{\dot{\epsilon}_0} \right) \right) \left(D - E \left(\frac{T - T_r}{T_m - T_r} \right)^m \right) \quad (12)$$

2.4. Modified Oxley's predictive machining theory

For the proposed orthogonal force model, cutting condition and material properties of both workpiece and tool are the inputs. The outputs are process related variables, such as shear angle, contact length, cutting forces, and shear flow stress along the tool-chip interface. The shear angle ϕ , strain rate constant C , and ratio of thickness of tool-chip interface plastic zone to chip thickness δ are selected based on the minimum force principle [OXLE89], then force and contact length. The main modifications are shown in the following sections. The required temperature information ($T_{shear-ave}$ and $T_{interface-ave}$) is calculated within every iteration based on other known process information as outlined in Section 2.2.

2.4.1. Along the primary shear zone AB

As shown in Appendix A that the angle of inclination of the resultant cutting force R to shear zone AB is given by

$$\tan \theta = 1 + 2 \left(\frac{\pi}{4} - \phi \right) - \frac{c\gamma_{AB}I}{k_{AB}} \quad (13)$$

The strain and the strain rate at AB can be given as by the relation [OXLE89]

$$\gamma_{AB} = \frac{1}{2} \frac{\cos \alpha}{\sin \phi \cos(\phi - \alpha)}, \quad \dot{\gamma}_{AB} = c \frac{V_s}{l} \quad (14)$$

Given γ_{AB} , $\dot{\gamma}_{AB}$, and $T_{shear-ave}$, as shown in Appendix A, the shear flow stress k_{AB} along the primary shear zone can be determined based on the modified Johnson-Cook equation, and the normal stress σ'_N can be found from the boundary condition at B for the normal stress distribution along AB:

$$\sigma'_N = k_{AB} \left(1 + \frac{\pi}{2} - 2\alpha - \frac{2c\gamma_{AB}I}{k_{AB}} \right) \quad (15)$$

2.4.2. Along the tool-chip interface

As discussed by Oxley [OXLE89], the maximum shear strain-rate at the tool-chip interface is:

$$\dot{\gamma}_{\text{int}} = \frac{V_{\text{chip}}}{\delta t_{\text{ch}}} \quad (16)$$

By balancing the moment about point B, similarly the tool-chip contact length is determined in this study as

$$h = \frac{t \sin \theta}{\cos \lambda \sin \phi} \left[1 + \frac{\frac{c \gamma_{AB} I}{k_{AB}}}{3 \left[1 + 2 \left(\frac{\pi}{4} - \phi \right) - \frac{c \gamma_{AB} I}{k_{AB}} \right]} \right] \quad (17)$$

The strain-hardening effect is considered as insignificant along the tool-chip interface [OXLE89]. Given $\dot{\gamma}_{\text{int}}$ and $T_{\text{interface-ave}}$, the shear flow stress in the chip adjacent to the interface can be calculated based on the modified Johnson-Cook equation as

$$k_{\text{ch}} = \frac{\sigma_{\text{ch}}}{\sqrt{3}} = \frac{1}{\sqrt{3}} \sigma_0 \left(1 + C \ln \frac{\dot{\gamma}_{\text{int}}}{\sqrt{3} \dot{\epsilon}_0} \right) \left(D - E \left(\frac{T_{\text{interface-ave}} - T_r}{T_m - T_r} \right)^m \right) \quad (18)$$

The stress distribution is assumed uniform along the tool-chip interface. The average normal stress σ_N and shear stress τ_{int} at the tool-chip interface are given by

$$\sigma_N = \frac{N}{hw}, \quad \tau_{\text{int}} = \frac{F}{hw} \quad (19)$$

2.4.3. Model solution

The shear angle ϕ is determined according to the fact that tool-chip interface shear stress τ_{int} resolved from the resultant cutting force for a given set of cutting conditions must be equal to the chip material shear flow stress k_{ch} , which is a function of strain, strain-rate, and temperature, at the interface for the same cutting condition. The search for the true value of ϕ will go through iterations until the calculated interface shear stress and the chip material shear flow stress is equal. If there is more than one shear angle that satisfies the above condition, the highest angle is chosen. The reasonable value C and δ are also searched iteratively at the same time, to simultaneously satisfy the condition:

$$\sigma_N = \sigma'_N \quad (20)$$

3. Model validation in hard turning with CBN tool

Although the basic approach presented herein was initially proposed to model the steady state cutting process with continuous chip [OXLE88], it is still practical to apply this approach to model the hard turning process with saw-tooth chip by considering the study by Ren *et al.* [RENH00] on machining of hardened P20 mold steel and the study by Shantla *et al.* [SHAT01] on the slot milling of H13 steel (46 HRc). The variation components of cutting forces due to chip segmentation are typically insignificant compared to the average force component [VYAS99], and the variation frequency is relatively high, around 10 to 100 KHz [DAVI96] [VYAS99].

To verify the proposed process model, experimental data from Ng. *et al.* [NGEG99] is considered here. The conditions for this orthogonally machining hardened steel process were: work piece material was AISI H13 steel (52 HRc); Tool was PCBN insert with -5° rake angle and $-20^\circ \times 0.2\text{mm}$ T-land chamfer; the cut was orthogonal with cutting speed of 75, 150, and 200m/min, undeformed chip thickness of 0.25mm, and width of cut of 2.0mm to satisfy the plain strain requirement. Since no flow stress information is available for AISI H13 steel (52 HRc), the modified Johnson-Cook equation for AISI H13 steel (46 HRc) [SHAT01] is used for this force modeling case. The constants of this modified Johnson-Cook equation are listed in Table 1. Other material physical properties for used tools and workpiece are listed in Table 2.

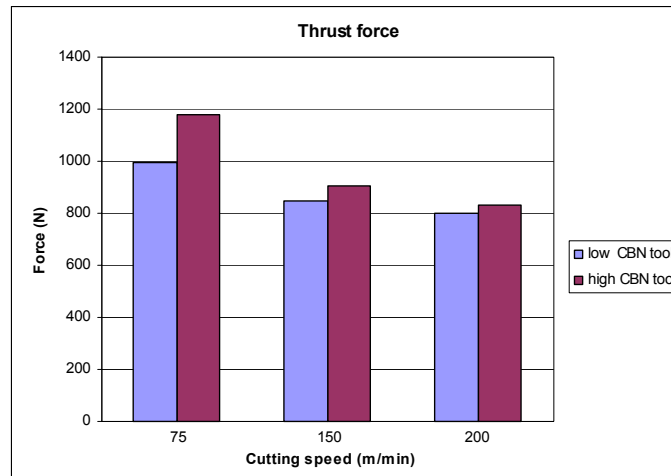
Since the applied feedrate is larger than chamfer length, the cutting zone is not only limited to chamfer land. There is a need to calculate the average rake angle as the input for the force model. Based on the approach of Manjunathaiiah and Endres on honed tool [MANJ96], the straight line connecting the base of the tool with the point on the rake face at the level of the free surface is used to calculate the average rake angle. For this particular experiment [NGEG99], the average rake angle is estimated as -19.9° for all three different cutting conditions.

A	B	C	D	E	m	n
674.8Mpa	239.2Mpa	0.027	1.16	0.88	1.3	0.28

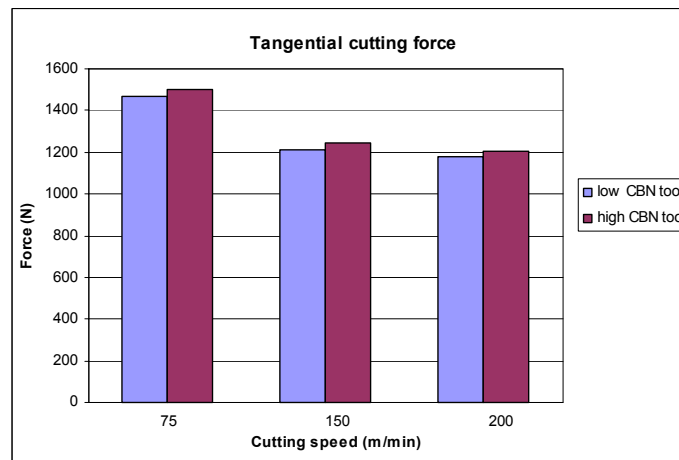
Table 1. Parameters of the modified Johnson-Cook equation for AISI H13 (46HRc) [SHAT01] (C,D,E, m , and n are dimensionless)

	Low CBN content tool [SHAT01]	High CBN content tool [SHAT01]	AISI H13 steel (46 HRc) [NGEG99]
Composition (vol%)	50% CBN, 40% TiC, 6% WC, 4% AlN/ AlB ₂	90% CBN, 10% AlN/ AlB ₂	
Density (Kg / m^3)	4370.1	3399.5	7760
Thermal conductivity ($W / m \cdot k$)	44	100	28.4
Specific heat capacity ($J / Kg \cdot k$)	750	960	$420+0.504 T$ (T in $^\circ C$)

Table 2. Composition and/or mechanical/physical property data for PCBN cutting tools and workpiece materials



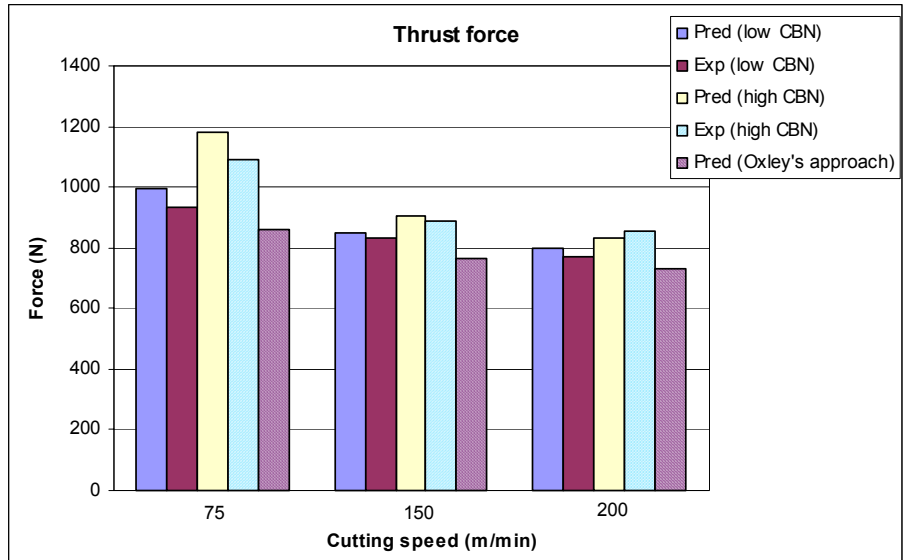
(a). Thrust force with cutting speed 75,150, and 200m/min



(b). Tangential cutting force with cutting speed 75,150, and 200m/min

Fig. 2. The predicted cutting forces when using different CBN content tool

The predicted cutting forces when using different CBN content tool are shown in Fig. 2 (a) and (b). It is observed that under the same cutting condition both the thrust and the tangential cutting forces generated by using high CBN content tool are larger than those by using low CBN content tool. The thrust force experiences a larger variation than that of tangential force between using low CBN content tool and high CBN content tool. Those observations agree with the experimental measurements [NGEG99] as shown on Fig. 3 (a) and (b). The force difference between the prediction and the measurement may have been attributed to (1). The workpiece material property of H13 steel with HRc 46 is used instead of H13 with HRc 52, and (2). The effective rake angle is estimated here and considered the same for all three cutting speeds.



(a). Thrust force with cutting speed 75,150, and 200m/min



(b). Tangential cutting force with cutting speed 75,150, and 200m/min

Fig. 3. Force comparison when using different CBN content tools

The predicted average temperature along the tool-chip interface is shown in Fig. 4. It can be seen that a higher temperature is reached along the tool-chip interface when a lower CBN content tool is used. It is suggested that the high temperature generated from using a low CBN content tool leads to low cutting forces in hard turning due to softening effect. The predicted temperature is compared with the FEM results [NGEG99] as shown in Fig. 5. Although the proposed model predicts larger temperature value along the tool-chip interface compared with FEM results, the results from the proposed model and FEM all show that a higher temperature is reached when using a lower CBN content tool.

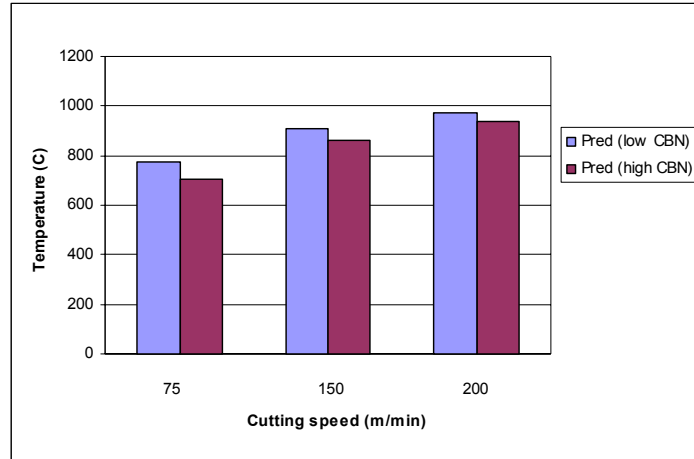


Fig. 4. Predicted temperature along the tool-chip interface using different CBN content tools

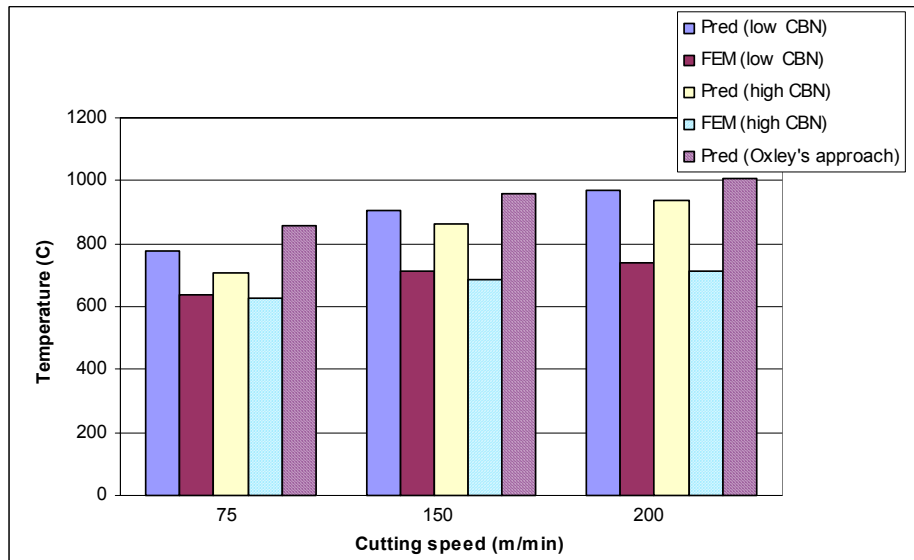


Fig. 5. Temperature comparison with FEM results [NGEG99] using different CBN content tools

Force and temperature predictions without considering tool thermal property are shown in Figs. 3 and 5 for comparison. The empirical thermal modeling methodology of Oxley's predictive machining theory [OXLE89] is used in this calculation. The modified Oxley's approach predicts higher thrust force than that of Oxley's approach, which may be the result of softening effect in view of a higher temperature as shown in Fig. 5. A better accuracy of thrust force modeling is observed within high cutting speed range from Fig. 3 (a).

4. Conclusion

By the thermal modeling of both the primary and the secondary heat sources, modification to Oxley's predictive machining theory is made to model the metal cutting behaviors. Temperature distribution along the primary and secondary shear zones is modeled with a moving heat source [HUAN02]. To generalize the modeling approach, the modified Johnson-Cook equation is

applied in the modified Oxley's approach to represent the workpiece material properties as a function of strain, strain rate, and temperature. Although the (modified) Johnson-Cook equation cannot capture blue brittle phenomenon and history effect, the prediction results from this study show that the Johnson-Cook equation works well as the material constitutive equation, at least within the normal machining condition range.

The proposed approach describes the effect of tool thermal property on cutting forces and it can facilitate tool design and process optimization. The model prediction is compared to the published experimental process data of hard turning AISI H13 steel (52 HRC) when using low CBN content tool and high CBN content tool. The proposed model and FEM both predict lower tangential and thrust forces and higher tool-chip interface temperature when using lower CBN content tool.

Appendix A. Modification to Oxley's predictive machining theory

The plane AB as drawn in Fig. 1 is an I-slipline and the variation normal stress p along it is given by [OXLE89]:

$$\frac{\partial p}{\partial s_1} + 2k \frac{\partial \psi}{\partial s_1} - \frac{\partial k}{\partial s_2} = 0 \quad (\text{A.1})$$

where ψ is the inclination of the slipline to some fixed axis and s_1 and s_2 are distances measured along and normal to the slipline. Assuming the distribution of p along AB is linear, the following relationship is derived [OXLE89];

$$\tan \theta = 1 + 2\left(\frac{\pi}{4} - \phi\right) - \left(\frac{dk}{ds_2}\right)_{AB} \frac{l}{2k_{AB}} \quad (\text{A.2})$$

$$\left(\frac{dk}{ds_2}\right)_{AB} = \left(\frac{dk}{d\gamma}\right)_{AB} \left(\frac{d\gamma}{dt}\right)_{AB} \left(\frac{dt}{ds_2}\right)_{AB} \quad (\text{A.3})$$

$$\left(\frac{d\gamma}{dt}\right)_{AB} = \dot{\gamma}_{AB} = c \frac{V_s}{l} \quad (\text{A.4})$$

$$\left(\frac{dt}{ds_2}\right)_{AB} = \frac{1}{V_c \sin \phi} \quad (\text{A.5})$$

Since $\varepsilon_{AB} = \frac{\gamma_{AB}}{\sqrt{3}}$ and $\dot{\varepsilon}_{AB} = \frac{\dot{\gamma}_{AB}}{\sqrt{3}}$, based on the modified Johnson-Cook equation

$$\begin{aligned} k_{AB} &= \frac{\sigma_{AB}}{\sqrt{3}} = \frac{1}{\sqrt{3}} \left(\sigma_0 + B \varepsilon_{AB}^n \left(1 + C \log \frac{\dot{\varepsilon}_{AB}}{\dot{\varepsilon}_0} \right) \left(D - E \left(\frac{T - T_r}{T_m - T_r} \right)^m \right) \right) \\ &= \frac{1}{\sqrt{3}} \left(\sigma_0 + B \left(\frac{\gamma_{AB}}{\sqrt{3}} \right)^n \right) \left(1 + C \log \frac{\dot{\gamma}_{AB}}{\sqrt{3} \dot{\varepsilon}_0} \right) \left(D - E \left(\frac{T - T_r}{T_m - T_r} \right)^m \right) \end{aligned} \quad (\text{A.6})$$

By assuming other variables are kept as constant, $\frac{\partial T}{\partial \gamma}$ is computed numerically based on discussed thermal model.

$$\begin{aligned} \left(\frac{dk}{d\gamma}\right)_{AB} &= \frac{\partial k}{\partial \varepsilon} \frac{\partial \varepsilon}{\partial \gamma} + \frac{\partial k}{\partial T} \frac{\partial T}{\partial \gamma} \\ &= \frac{1}{3} \left(Bn \varepsilon_{AB}^{n-1} \right) \left(1 + C \log \frac{\dot{\varepsilon}_{AB}}{\dot{\varepsilon}_0} \right) \left(1 - \left(\frac{T_{AB} - T_r}{T_m - T_r} \right)^m \right) + \\ &\quad \frac{1}{\sqrt{3}} \left(\sigma_0 + B \varepsilon_{AB}^n \right) \left(1 + C \log \frac{\dot{\varepsilon}_{AB}}{\dot{\varepsilon}_0} \right) \left(-m \left(\frac{T_{AB} - T_r}{T_m - T_r} \right)^{m-1} \right) \frac{\partial T}{\partial \gamma} \end{aligned} \quad (A.7)$$

Donating $I = \left(\frac{dk}{d\gamma}\right)_{AB}$, using Equ. (14) and

$$V_s = \frac{V_c \cos \alpha}{\cos(\phi - \alpha)} \quad (A.8)$$

$$\text{So, } \left(\frac{dk}{ds_2}\right)_{AB} = (I) \left(c \frac{V_s}{l} \right) \left(\frac{1}{V_c \sin \phi} \right) = \frac{2c\gamma_{AB}I}{l} \quad (A.9)$$

The following relationship can be derived as

$$\begin{aligned} \tan \theta &= 1 + 2 \left(\frac{\pi}{4} - \phi \right) - \left(\frac{dk}{ds_2}\right)_{AB} \frac{l}{2k_{AB}} \\ &= 1 + 2 \left(\frac{\pi}{4} - \phi \right) - \frac{c\gamma_{AB}I}{k_{AB}} \end{aligned} \quad (A.10)$$

Similarly, the normal stress acting on the tool-chip interface at point B can be determined as:

$$\sigma'_N = k_{AB} \left(1 + \frac{\pi}{2} - 2\alpha - \frac{2c\gamma_{AB}I}{k_{AB}} \right) \quad (A.11)$$

References:

- [BARR01] Barry, J., and Byrne, G., "Cutting Tool Wear in the Machining of Hardened Steel, Part 2: Cubic Boron Nitride Cutting Tool Wear", *Wear*, Vol. (247), 2001, pp. 139-151.
- [DAVI96] Davies, M.A., Chou, Y., and Evans, C. J., "On Chip Morphology, Tool Wear and Cutting Mechanics in Finish Hard Turning", *Annals of CIRP*, Vol. (45)(1), 1996, pp. 77-82.
- [HUAN02] Huang, Y., and Liang, S.Y., "Cutting Temperature Modeling Based on Non-uniform Heat Intensity and Partition Ratio", submitted to *Inter. J. of Machine Tools and Manufacture*, 2002
- [JOHN85] Johnson, G.R., and Cook, W.H., "Fracture characteristic of Three Metals Subjected to Various Strains, Strain-rate, Temperature, and Pressure", *Eng. Fracture Mechanics*, Vol. (21), 1985, pp. 31-48.
- [KLAM73] Klamecki, B.E., "Incipient Chip Formation in Metal Cutting – A Three Dimension Finite Element Analysis", Ph.D. dissertation, Univ. of Illinois, 1973.
- [KONI93] Konig, W., Berkold, A., and Koch, K.F., "Turning vs. Grinding", *Annals of CIRP*, Vol. (42)(1), 1993, pp. 39-43.

- [LEEE51] Lee, E.H., and Shaffer, B.W., "Theory of Plasticity Applied to Problems of Machining", ASME J. of App. Mechanics, Vol. (18)(4), 1951, pp. 104-113.
- [LOEW54] Loewen, E.G., and Shaw, M.C., "On the Analysis of Cutting Tool Temperatures", Trans. ASME, Vol. (76), 1954, pp. 217-231.
- [MERC45] Merchant, M.E., "Mechanics of the Metal Cutting Process, Part 2: Plasticity Conditions in Orthogonal Cutting", J. Appl. Phys., Vol. (16), 1945, pp. 318-324.
- [MEYE94] Meyers, M.A., Dynamic Behavior of Materials, John Wiley & Sons, NY, 1994.
- [NGEG99] Ng, E.G., Aspinwall, D.K., Brazil, D., and Monaghan, J., "Modeling of Temperature and Forces when Orthogonally Machining Hardened Steel", Int. J. Mach. Tools Manufact., Vol. (39), 1999, pp. 885-903.
- [MANJ96] Manjunathaiah, J., and Endres, W.J., "Effects of a Honed Cutting Edge in Machining", in Proceeding of the 2nd S.M. Wu Manufacturing Symposium, Ann Arbor, MI, 1996, pp. 25-32.
- [OXLE88] Oxley, P.L.B., "Modelling Machining Processes with a View to Their Optimization and to the Adaptive Control of Metal Cutting Machine Tools", Robotics & Computer-Integrated Manufacturing, Vol. (4)(1/2), 1988, pp. 103-119.
- [OXLE89] Oxley, P.L.B., Mechanics of Machining, an Analytical Approach to Assessing Machinability, Ellis Horwood Limited, West Sussex, England, 1989.
- [POUL01] Poulachon, G., and Moisan, A., and Jawahir, I.S., "On Modeling the Influence of Thermo-Mechanical Behavior in chip Formation during Hard Turning of 100Cr6 Bearing Steel", Annals of CIRP, Vol. (50)(1), 2001, pp. 31-36.
- [RENH00] Ren, H, and Altintas, Y., "Mechanics of Machining with Chamfered Tools", ASME J. of Manuf. Sci and Eng., Vol. (122)(4), 2000, pp. 650-659.
- [SHAT01] Shatla, M., Kerk, C., and Altan, T, "Process Modeling in Machining, Part 1: Determination of Flow Stress Data", Inter. J. Mach. Tools & Manuf, Vol. (41), 2001, pp. 1511-1534.
- [SHAW93] Shaw, M.C., and Vyas, A., "Chip Formation in the Machining of Hardened Steel", Annals of CIRP, Vol. (42)(1), 1993, pp. 29-33.
- [VYAS99] Vyas, A., and Shaw, M.C., "Mechanics of Saw-Tooth Chip Formation in Metal Cutting", ASME J. of Manufacturing Sci. and Eng., Vol. (121), 1999, pp. 163-172.
- [WANG88] Wang, B. P., Sadat, A. B., and Twu, M. J., "Finite Element Simulation of Orthogonal Cutting – A Survey", Materials in manufacturing processes, MD-vol. (8), Dec. 1988, ASME WAM, Chicago, IL, pp. 87-91.